Supplementing information

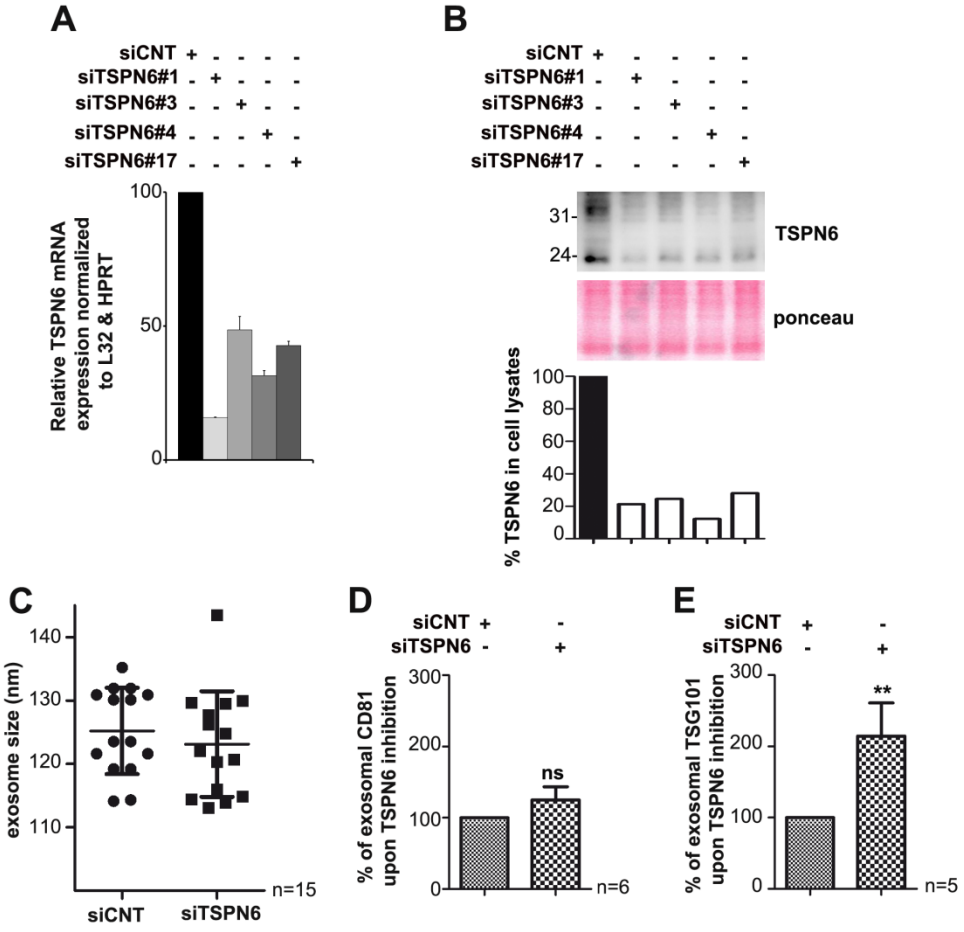

Fig. S1: Validation of TSPN6 siRNAs and effect of TSPN6-inhibition on exosome size and composition. A. TSPN6 mRNA levels were measured by quantitative RT-PCR and expressed in arbitrary units as compared to HPRT and L32 signals (as controls). Expression of TSPN6 in MCF-7 cells treated with 4 different RNAi (siTSPN6#1, siTSPN6#3, siTSPN6#4 and siTSPN6#17) normalized to control cells (siCNT). **B.** TSPN6 protein levels in MCF-7 cells treated with 4 different RNAi (siTSPN6#1, siTSPN6#3, siTSPN6#4 and siTSPN6#17) compared to control cells (siCNT), as detected by Western blot. **C.** Exosomes were analyzed by Nanosight. TSPN6 was depleted using two different RNAi (siTSPN6#1 and siTSPN6#4). The two TSPN6 siRNAs were tested separately, in parallel cultures, and the results of both were pooled. Each point represents the size of exosomes from three independent measurements. The value 'n' indicates the number of independent experiments. **D-E.** Exosomes secreted by TSPN6-depleted cells (siTSPN6) and control exosomes (siCNT) were isolated by ultracentrifugation. Exosomes were analyzed by Western blot, testing for CD81 (D) and TSG101 (E) markers, as indicated. Of note, loss of syndecan/CD63/syntenin does not affect exosomal TSG101[1], but loss of TSG101 leads to early endosome tubulation[2] and decreases exosome release, including the release of syntenin exosomes[1]. Histograms represent mean signal intensities ± SEM in exosomes relative to signals obtained for control exosomes. Values were calculated from n independent experiments as indicated. ** $P < 0.01$, n.s. non significant (Student's t-test).

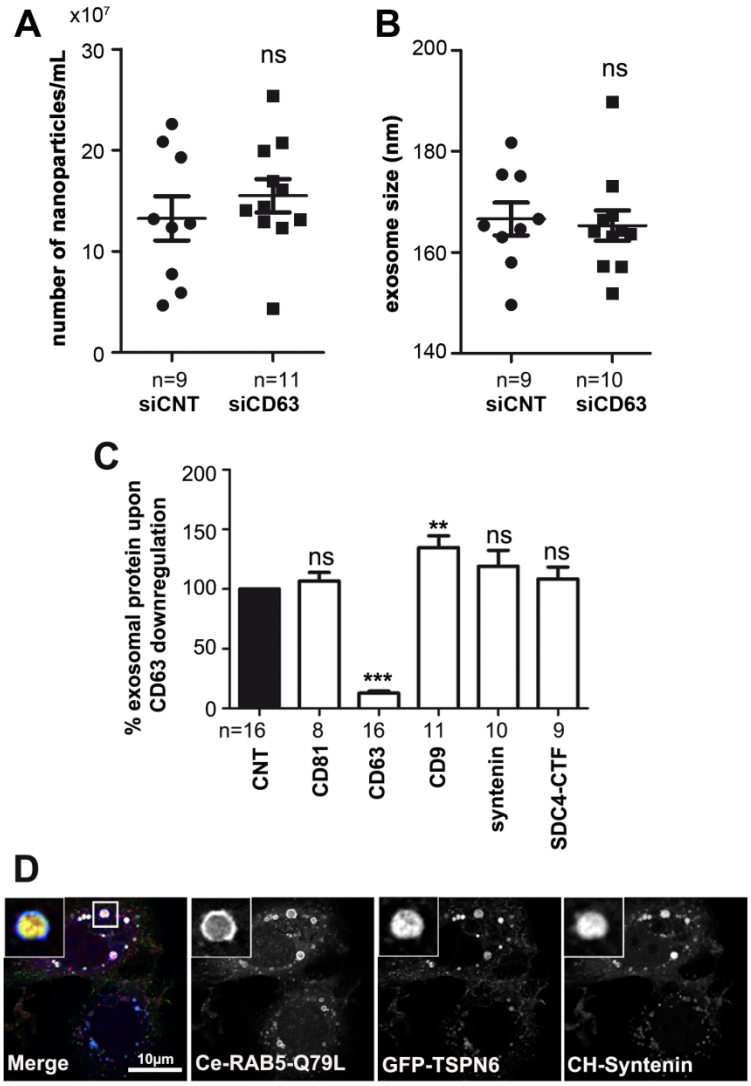

Fig. S2: CD63 inhibition does not increase (syntenin) exosomal releases. A-C. Exosomes secreted by CD63-depleted cells (siCD63#1, siCD63#2, siCD63#4), and control cells (siCNT) were isolated by ultracentrifugation. Exosomes were analyzed by Nanosight (**A, B**) or by Western blot, testing for several markers, as indicated (**C**). **A-B.** The different siRNAs were tested separately, in parallel cultures, and the results were pooled. Each point represents the number (**A**) or the size (**B**) of exosomes from n independent measurements. Histograms represent mean signal intensities ± SEM in exosomes secreted by CD63-depleted cells, relative to signals obtained for control exosomes. SDC4-CTF; syndecan-4 C-terminal fragment. ** $P < 0.01$, *** $P < 0.001$, n.s. non-significant (Student's t-test). The value 'n' indicates the number of independent experiments. **D**. Confocal micrographs of MCF-7 cells transiently transfected for 24h with expression vectors for Ce-rab5-QL, GFP-TSPN6 and mCh-syntenin. Note the concentration of mCh-syntenin and GFP-TSPN6 inside the lumen of the enlarged endosomes outlined by Ce-rab5-QL (see insets for higher magnification of individual endosomes). n, number of independent experiments.

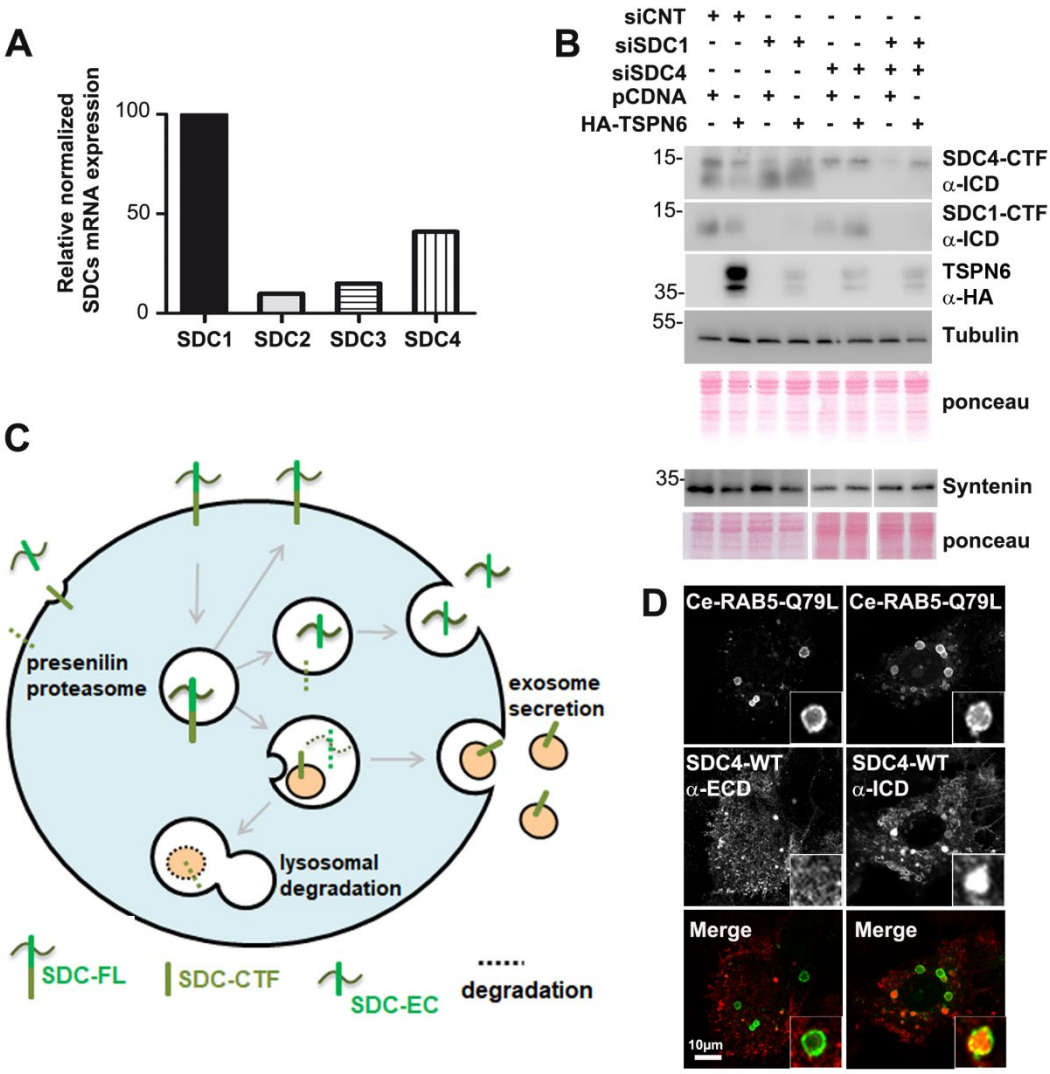

Fig. S3: SDCs expression in MCF7 cells, validation of SDC1 and SDC4 siRNAs and diagram of SDC4 intracellular and extracellular turnover. A. mRNA levels of the 4 SDCs were measured by quantitative RT-PCR and expressed in arbitrary units as compared to HPRT and L32 signals (as controls). Expression of the 4 SDCs in MCF-7 cells normalized to the level of SDC1. **B.** Validation of SDC1 and SDC4 siRNAs. MCF-7 cells treated with siRNA targeting SDC1 (siSDC1) or SDC4 (siSDC4) or control cells (siCNT) and overexpressing TSPN6 (HA-TSPN6) or the control (empty vector) were analyzed for SDC1, SDC4, TSPN6, tubulin and sytenin protein levels, as detected by Western blot. **C**. Scheme illustrating syndecan-4 turnover. Upon SDC4-FL cleavage by Matrix Metalloproteinases **(**MMPs), two discrete products are generated: SDC4-CTF, migrating around 15 kDa and SDC4-EC, the corresponding fragment of the SDC4-ectodomain, migrating around 25 kDa after digestion of the heparan sulfate (HS) chains. The latter is solely detectable in the culture medium. Note that several different extracellular and luminal proteases may generate SDC-CTFs, including proteases that fail to yield a discrete ectodomain fragment. SDC4-ectodomain can be shed, but also be degraded by lysosomal enzymes (proteases and glycosidases). **D**. Confocal micrographs of MCF-7 cells transiently transfected for 24h with expression vectors for Ce-rab5-QL (green) and SDC4-WT (red) and stained with SDC4 α-ECD or α-ICD antibodies. Note the concentration of SDC4 stained with α-ICD antibody inside the lumen of the enlarged endosomes outlined by Ce-rab5-QL (see insets for higher magnification of individual endosomes).

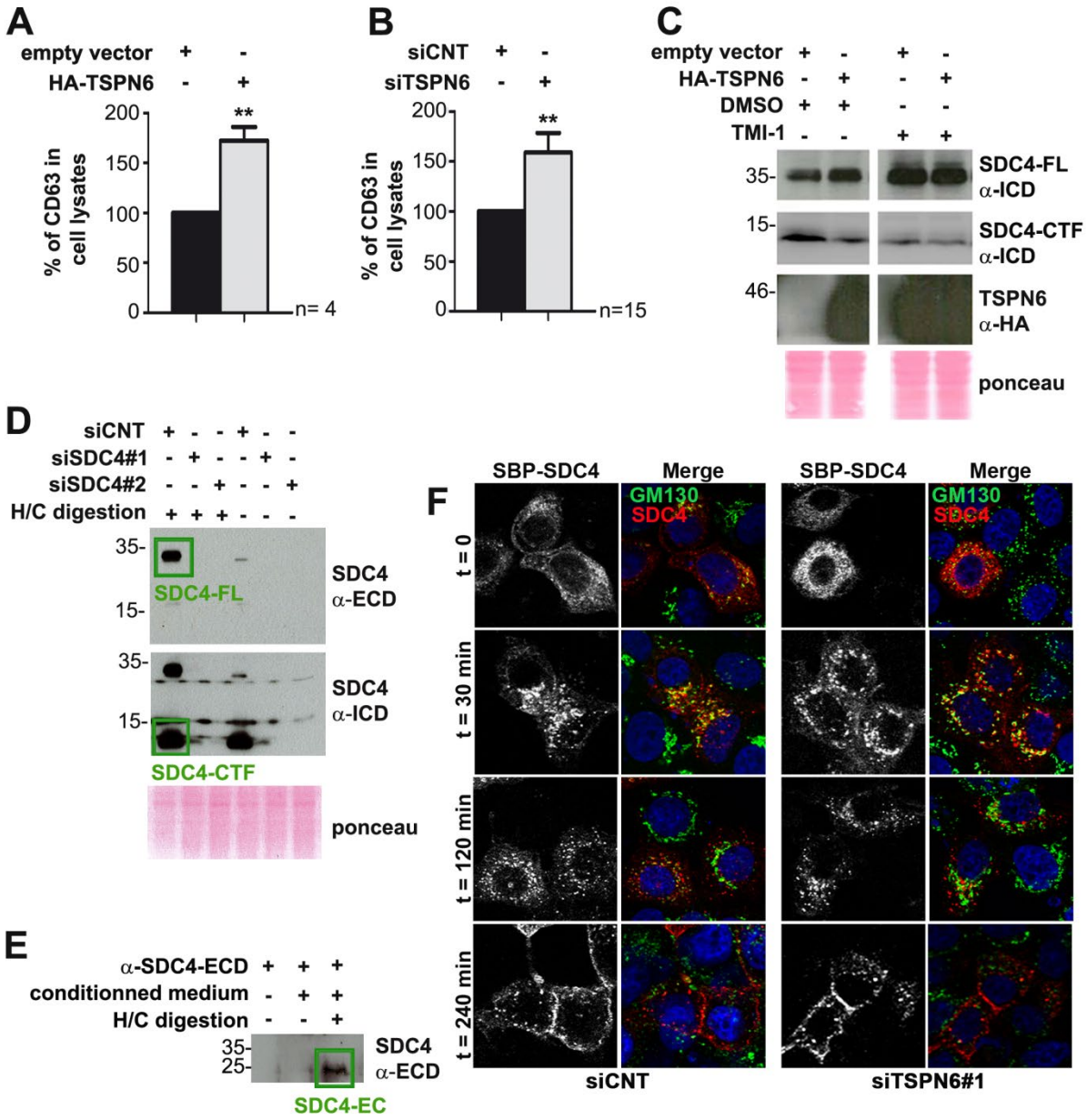

Fig. S4: CD63 cellular levels upon TSPN6 overexpression and downregulation. Tetraspanin-6 silencing does not block syndecan-4 trafficking from the ER, via the Golgi, to the plasma membrane. A. MCF-7 cells overexpressing TSPN6 (HA-TSPN6) and control cells (empty vector) were analyzed for CD63 levels in total cell lysates, by Western blot. Histograms represent the mean signal intensity for CD63 ± SEM in total cell lysates relative to signals in control cells. **B**. TSPN6-depleted MCF-7 cells (siTSPN6, the four TSPN6 siRNAs were tested separately, in parallel cultures, and the results were pooled) and control cells (siCNT) were analyzed for CD63 levels in total cell lysates, by Western blot. Histograms represent the mean signal intensity for CD63 ± SEM, relative to the signal in control cells. Note that, like the levels of SDC4-FL in cells, the cellular levels of CD63 increase upon both the over-expression and the down-regulation of TSPN6. **C.** Western blot analysis of MCF-7 cells overexpressing TSPN6 (HA-TSPN6) for 24h and control cells (empty vector) were treated with TMI-1 (inhibitor of matrix metalloproteinase (MMPs) and ADAM17; 10 µM) or DMSO as control. **D**. Cellular syndecan-4. Cells silenced for SDC4 expression using two different siRNA (siSDC4#1 and siSDC4#2) and control cells (siCNT)

were subjected to heparitinase/chondroitinase (H/C) digestion, or not, before analysis by Western blot with the indicated antibodies (α–). ECD; extracellular domain, ICD; intracellular domain, SDC4-FL; full length syndecan-4, SDC4-CTF; syndecan-4 C-terminal fragment. **E.** Shed syndecan-4. Culture media from MCF-7 cells were analyzed for the presence of shed cleaved SDC4 ectodomain (25 kDa form) by immunoprecipitation experiments using the antibody recognizing the ECD. Heparan and chondroitin sulfate chains were digested with heparitinase/chondroitinase (H/C) when indicated. **F. Rush experiment.** MCF-7 cells were treated with TSPN6 RNAi (siTSPN6#1) or non-targeting RNAi (siCNT) for 48 hours and then transiently transfected for 24h with an expression vector for Streptavidin Binding Protein fused to SDC4 (SBP-SDC4). SBP-SDC4 is retained in the ER and is allowed to leave the ER upon biotin addition. Representative confocal micrographs of control (siCNT) and TSPN6-depleted (siTSPN6#1) MCF-7 cells overexpressing SBP-SDC4 (red). Cells were treated with biotin for different periods of time as indicated. At 30 min after biotin addition, SBP-SDC4 (red) extensively co-localizes with the Golgi marker GM130 (green; yellow in merge). At 240 minutes after biotin addition, SBP-SDC4 has reached the plasma membrane, similarly in both control cells (siCNT) and in TSPN6-depleted cells (siTSPN6#1).

SI Materials and Methods

Mass spectrometry analysis Four biological replicates (GFP-TSPN6 versus GFP) were used for label free LC MSMS relative quantitation. Each replicate was further injected thrice on the system. Briefly, pulldown protein extracts were loaded on NuPAGE 4-12% Bis-Tris acrylamide gels (Life Technologies) to stack proteins in a single band that was stained with Imperial Blue (Pierce, Rockford, IL) and cut from the gel. Gels pieces were submitted to an in-gel trypsin digestion according to Shevchenko, A [3]. Briefly, gel pieces were washed and destained using 100 mM NH4HCO3/acetonitrile (50/50). Destained gel pieces were shrunk with acetonitrile and were rehydrated in the presence of 100 mM ammonium bicarbonate in 50% acetonitrile and dried at room temperature. Protein bands were then rehydrated and cysteines were reduced using 10 mM DTT in 100 mM ammonium bicarbonate pH 8.0 for 45 min at 56 C before alkylation in the presence of 55 mM iodoacetamide in 100 mM ammonium bicarbonate pH 8.0 for 30 min at room temperature in the dark. Proteins were then washed twice in 100 mM ammonium bicarbonate and finally shrunk by incubation for 5 min with 100 mM ammonium bicarbonate in 50% acetonitrile. The resulting alkylated gel pieces were dried at room temperature. The dried gel pieces were swollen by incubation in 100 mM ammonium bicarbonate pH 8.0 supplemented with trypsin (12.5 ng/µL; Promega) for 1 h at 4 C and then incubated overnight at 37°C. Peptides were harvested by collecting the initial digestion solution and carrying out two extractions; first in 5% formic acid and then in 5% formic acid in 60% acetonitrile. Pooled extracts were dried down in a centrifugal vacuum system. Samples were reconstituted with 0.1% trifluoroacetic acid in 4% acetonitrile and analyzed by liquid chromatography (LC)-tandem mass spectrometry (MS/MS) using an Orbitrap Fusion Lumos Tribrid Mass Spectrometer (Thermo Electron, San Jose, CA) online with a nanoRSLC Ultimate 3000 chromatography system (Dionex, Sunnyvale, CA). Peptides were separated on a 50 cm Dionex Acclaim PepMap RSLC C18 column. For peptide

ionization in the EASY-Spray nanosource in front of the Orbitrap Fusion Lumos Tribrid Mass Spectrometer, spray voltage was set at 2.2 kV and the capillary temperature at 275 °C. The Orbitrap Lumos was used in data dependent mode to switch consistently between MS and MS/MS. Time between Masters Scans was set to 3 seconds. MS spectra were acquired with the Orbitrap in the range of m/z 400-1600 at a FWHM resolution of 120 000 measured at 400 m/z. AGC target was set at 4.0e5 with a 50 ms Maximum Injection Time. For internal mass calibration the 445.120025 ions was used as lock mass. The more abundant precursor ions were selected and collision-induced dissociation fragmentation was performed in the ion trap to have maximum sensitivity and yield a maximum amount of MS/MS data. Number of precursor ions was automatically defined along run in 3s windows using the "Inject Ions for All Available parallelizable time option" with a maximum injection time of 300 ms. The signal threshold for an MS/MS event was set to 5000 counts. Charge state screening was enabled to exclude precursors with 0 and 1 charge states. Dynamic exclusion was enabled with a repeat count of 1 and duration of 60 s.

Quantitative analysis The iBAQ [4] intensity were processed using the freely available MaxQuant computational proteomics platform, version 1.6.3.4 [5,6]. The acquired raw LC Orbitrap MS data were first processed using the integrated Andromeda search engine [7]. Spectra were searched against the human database subset of the SwissProt database (date 180919, 20394 entries). This database was supplemented with a set of 245 frequently observed contaminants. The following parameters were used for searches: (i) trypsin allowing cleavage before proline; (ii) two missed cleavages were allowed; (ii) monoisotopic precursor tolerance of 20 ppm in the first search used for recalibration, followed by 4.5 ppm for the main search and 0.5 Da for fragment ions from MS/MS ; (iii) cysteine carbamidomethylation (+57.02146) as a fixed modification and methionine oxidation (+15.99491) and N-terminal acetylation (+42.0106) as variable modifications; (iv) a maximum of five modifications per

peptide allowed; and (v) minimum peptide length was 7 amino acids and a maximum mass of 4,600 Da. The match between runs option was enabled to transfer identifications across different LC-MS/MS replicates based on their masses and retention time within a match time window of 0.7 min and using an alignment time window of 20 min. The quantification was performed using a minimum ratio count of 1 (unique+razor) and the second peptide option to allow identification of two co-fragmented co-eluting peptides with similar masses. The false discovery rate (FDR) at the peptide and protein levels were set to 1% and determined by searching a reverse database. For protein grouping, all proteins that cannot be distinguished based on their identified peptides were assembled into a single entry according to the MaxQuant rules. The statistical analysis was done with Perseus program (version 1.6.1.3) from the MaxQuant environment (www.maxquant.org). The iBAQ intensity were uploaded from the ProteinGroups.txt file. The iBAQ intensities are roughly proportional to the molar quantities of the proteins. Proteins marked as contaminant, reverse hits, and "only identified by site" were discarded. Quantifiable proteins were defined as those detected in 100% of samples in at least one condition (GFP-Tetraspanin6 or GFP Pool Down). Protein intensities were base 2 logarithmized to obtain a normal distribution. Missing values were replaced using data imputation by randomly selecting from a normal distribution centered on the lower edge of the intensity values that simulates signals of low abundant proteins using default parameters (a downshift of 1.8 standard deviation and a width of 0.3 of the original distribution). In this way, imputation of missing values in the controls allows statistical comparison of protein abundances that are present only in the positive Tetraspanin 6 samples. To determine whether a given detected protein was specifically differential a two-sample t-test were done using permutation based FDR-controlled at 0.01 and employing 250 permutations. The p value was adjusted using a scaling factor s0 with a value of 1 [8]. The differential proteomics analysis was carried out on identified proteins after removal of

proteins only identified with modified peptides, peptides shared with other proteins, proteins from contaminant database and protein which are present above 100% in at least one condition.

The mass spectrometry proteomics data, including search results, have been deposited to the ProteomeXchange Consortium (www.proteomexchange.org) [9] via the PRIDE [10] partner repository with the dataset identifier PXD014559.

Supplementary references

1. Baietti, M. F. *et al.* Syndecan-syntenin-ALIX regulates the biogenesis of exosomes. *Nat Cell Biol* **14**, 677–685 (2012).
2. Razi, M. & Futter, C. E. Distinct roles for Tsg101 and Hrs in multivesicular body formation and inward vesiculation. *Mol. Biol. Cell* **17**, 3469–3483 (2006).
3. Shevchenko, A., Wilm, M., Vorm, O. & Mann, M. Mass spectrometric sequencing of proteins silver-stained polyacrylamide gels. *Anal. Chem.* **68**, 850–858 (1996).
4. Schwanhäusser, B. *et al.* Global quantification of mammalian gene expression control. *Nature* **473**, 337–342 (2011).
5. Cox, J. *et al.* Accurate proteome-wide label-free quantification by delayed normalization and maximal peptide ratio extraction, termed MaxLFQ. *Mol. Cell Proteomics* **13**, 2513–2526 (2014).
6. Cox, J. & Mann, M. MaxQuant enables high peptide identification rates, individualized p.p.b.-range mass accuracies and proteome-wide protein quantification. *Nat. Biotechnol.* **26**, 1367–1372 (2008).
7. Cox, J. *et al.* Andromeda: a peptide search engine integrated into the MaxQuant environment. *J. Proteome Res.* **10**, 1794–1805 (2011).
8. Tusher, V. G., Tibshirani, R. & Chu, G. Significance analysis of microarrays applied to the ionizing radiation response. *Proc. Natl. Acad. Sci. U.S.A.* **98**, 5116–5121 (2001).

9. Vizcaíno, J. A. *et al.* ProteomeXchange provides globally coordinated proteomics data submission and dissemination. *Nat. Biotechnol.* **32**, 223–226 (2014).

10. Vizcaíno, J. A. *et al.* 2016 update of the PRIDE database and its related tools. *Nucleic Acids Res.* **44**, 11033 (2016).